lubricants

MDPI

Article

Accelerated Wear Test Design Based on Dissipation Wear Model Entropy Analysis under Mixed Lubrication

Hongju Li, Ying Liu *, Haoran Liao and Zhurong Liang

State Key Laboratory of Tribology, Tsinghua University, Beijing 100084, China;
hj-li18@mails.tsinghua.edu.cn (H.L.); liaohaoran916@yeah.net (H.L.); liangzr20@mails.tsinghua.edu.cn (Z.L.)
* Correspondence: liuying@mail.tsinghua.edu.cn

Abstract: Theoretical life prediction of tribo-pairs such as seals, bearings and gears with the failure form of wear under mixed lubrication depends on quantitative analysis of wear. Correspondingly, the wear life test depends on an accelerated wear test method to save the time and financial costs. Therefore, the theoretical basis of accelerated test design is a wear model providing a quantitative relationship between equivalents and accelerated test duration. In this paper, an accelerated wear test design method based on dissipation wear model entropy analysis under mixed lubrication is proposed. Firstly, the dissipation wear model under mixed lubrication is verified by standard experiments as a theoretical basis. Then, an accelerated wear test design method is proposed, taking the entropy increase in the dissipation wear model as an equivalent. The verification test shows that 20 times acceleration could be reached by adjustment of the entropy increase rate. The effect of entropy increase rate gradient of duty parameters is also discussed, revealing the fastest acceleration direction. Finally, the advantages and disadvantages of the proposed method are discussed. The results in this paper are expected to contribute to long life predictions of tribo-pairs.

Keywords: accelerated wear test; dissipation wear model; mixed lubrication; entropy increase; gradient

Citation: Li, H.; Liu, Y.; Liao, H.; Liang, Z. Accelerated Wear Test Design Based on Dissipation Wear Model Entropy Analysis under Mixed Lubrication. *Lubricants* **2022**, *10*, 71. https://doi.org/10.3390/lubricants10040071

Received: 2 March 2022
Accepted: 14 April 2022
Published: 16 April 2022

1. Introduction

Life prediction of machine elements under working conditions is a basic issue in technology and engineering. With the increasing of engineering applications, major equipment such as the aero-engine, nuclear coolant pump, and gas turbine are working under more complicated working conditions and higher duty parameters [1,2], leading to harsh environments for key mechanical parts with tribo-pairs under mixed lubrication, including seals [3,4], bearings [5] and gears [6]. For example, the relative sliding velocity and temperature of seals in an aero-engine could be over 180 m/s and 620 °C, respectively [7,8]. Due to such strict conditions, the wear level is aggravated; thus, the probability of wear failure has been increased remarkably and becomes the main failure form for these key mechanical parts [9,10]. It is estimated that 70–80% failures of seals in aero-engines are the result of wear [2,7,8]. Considering that wear failure is the main limit for the life of these mechanical parts, it is reasonable to predict life from the perspective of wear prediction.

An appropriate and accurate wear model is required to predict the wear amount with certain duty parameters and wear duration. More than 300 kinds of quantitative wear models have been proposed with consideration of over 100 kinds of influence factors to date [11,12]. Among these models, the dissipation wear model based on the frictional thermodynamics proves accurate wear prediction [13,14]. In terms of physical concepts, the wear process is regarded as an irreversible thermodynamic degradation process of the material and is evaluated by entropy increase, conforming to the physical intrinsic properties of wear [15–21]. As for mathematical form, a brief linear relationship between wear amount and entropy increase between solids is revealed under different lubrication conditions, including dry friction, grease lubrication, boundary lubrication, and mixed

lubrication [5,22–26]. In addition, the wear process at a micro scale could be described by a dissipation wear model, presenting multi-scale properties [27,28]. Hence, the dissipation wear model is selected as the fundamental theoretical model in this paper.

Another issue for wear life prediction is the constantly increasing wear life test duration due to progressions in abrasive resistance technologies such as surface modification [29], structure modification [30] and new materials [31], although the available test time is generally limited to a much shorter duration than the wear life under common duty parameters [32–34]. Hence, long life test duration of a traditional 1:1 simulation test with relatively low duty parameters could not be acceptable [32–34]. The accelerated wear test methods are required to shorten the life test duration instead.

The key of the accelerated wear test is selecting an appropriate physical or mathematical quantity as the equivalent of wear, meaning a quantitative relationship should be revealed between such equivalent and wear amount. By modifying the 'stress levels' of the duty parameters, the rate of the equivalent could be increased, resulting in increasing of the wear rate and acceleration of the test duration. A few equivalents of wear have been investigated, including failure probability [35–37], surface topography [38] and temperature [39,40]. However, existing accelerated wear test methods have not been investigated with quantitative wear models as basics yet, leading to an insufficiency in theoretical supports and feasibility.

For this reason, an accelerated wear test method based on a dissipation wear model is proposed in this paper. Both theoretical deduction and experimental verification are presented for the following contents: a dissipation wear model under mixed lubrication condition, an accelerated wear test method based on this quantitative model, and design of the test based on entropy gradient analysis.

2. Theoretical Basis

2.1. Dissipation Wear Model

Based on tribology system theory, wear has been defined as an irreversible thermodynamics process that could be evaluated by the entropy increase [41,42]. Such theory is referred to as frictional thermodynamics, of which the core is the entropy equilibrium equation (Equation (1)), providing a theoretical basis for the dissipation wear model.

$$\dot{S} = \dot{S}_{gen} + \dot{S}_f \tag{1}$$

It is revealed in Equation (1) that the entropy variation rate is the sum of entropy source rate $\dot{S}_{gen}$ and entropy flow rate $\dot{S}_f$. Four entropy source items are successively listed in Equation (2), including heat conduction, diffusion, viscous flow and chemical reaction. Similarly, three entropy flow items are successively listed in Equation (3), including convection, heat conduction and diffusion [41,42].

$$\dot{S}_{gen} = J_q \nabla\left(\frac{1}{T}\right) + \sum_i J_i\left[-\nabla\left(\frac{\mu_i}{T}\right) + \frac{M_i F_i}{T}\right] - \frac{1}{T}\prod \nabla U + \sum_\rho \frac{A_\rho}{T}\omega_\rho \tag{2}$$

$$\dot{S}_f = SU + \frac{J_q}{T} - \sum_i \frac{\mu_i}{T} J_i \tag{3}$$

Local equilibrium assumption is applied in frictional thermodynamics, regarding the entropy variation in each micro unit as zero so that a quasi-static state could be presented by the whole system. Accordingly, the numerical value of the entropy source rate $\dot{S}_{gen}$ is equal to that of the entropy flow rate $\dot{S}_f$ [41,42].

$$\dot{S}_{gen} = -\dot{S}_f \tag{4}$$

The entropy flow rate $\dot{S}_f$ could be approximately presented as the heat condition $\dot{Q}$ under a phenomenological view.

$$\dot{S}_f = \frac{\dot{Q}}{T_{bulk}} \tag{5}$$

Based on both the frictional thermodynamics above and experimental evidence that the degradation rate of the material is proved to be in direct proportion with a coefficient of B to the entropy flow rate [39,40], the dissipation wear model could be established since wear is a typical degradation form of the material (see Equation (6)).

$$\dot{w}_v = B\frac{\dot{Q}}{T_{bulk}} \tag{6}$$

Since the heat production $\dot{Q}$ in a tribology system mainly originates from frictional heat, a further expression of Equation (6) could be shown as Equation (7).

$$\dot{w}_v = B\frac{\mu N v}{T_{bulk}} \tag{7}$$

Equations (6) and (7) have been verified by wear experiments under dry friction and grease lubrication conditions. However, lubrication conditions will experience a transforming process through boundary lubrication, mixed lubrication and hydrodynamic lubrication with the changing of duty parameters when it comes to circumstances with fluid lubricants [43]. Normal loads in such conditions are shared by solid asperities contact and fluid lubricant films; accordingly, the concept of 'load sharing' is raised to describe the load share proportion of solid and fluid. A load sharing factor ξ is introduced into the dissipation wear model as a modification [25,26].

$$\dot{w}_v = \xi B\frac{\mu N v}{T_{bulk}} \tag{8}$$

Considering the characteristics of different lubrication conditions, the load-sharing factor ξ_n at the transforming point between boundary lubrication and mixed lubrication is valued as 1, while the load-sharing factor ξ_0 at the transforming point between mixed lubrication and hydrodynamic lubrication is valued as 0 [25,26]. The load-sharing factor ξ_i under a mixed lubrication condition could be obtained with an interpolation of friction coefficients, μ_n, μ_0 and μ_i in the Stribeck curve [43–45], respectively, at the two transforming points and the aimed point in a mixed lubrication regime.

$$\frac{\xi_n - \xi_i}{\mu_n - \mu_i} = \frac{\xi_n - \xi_0}{\mu_n - \mu_0} \tag{9}$$

In summary, the dissipation wear model that connects the wear and entropy increases with a linear relationship under mixed lubrication is presented in this section.

2.2. Accelerated Wear Test Method

In the accelerated wear test method, it is suggested that different wear processes with the same equivalent amount E could be considered as equal [35–40]. If a wear process reaches an equivalent amount E with equivalent function $E_i(t)$ in duration t_0 under a common parameter level, the acceleration effect could be realized by reaching the same E in a shorter duration t_i with an equivalent function $E_0(t)$ under a higher parameter level.

$$E_i(t_i) = E_0(t_0) \tag{10}$$

The Acceleration Factor (*AF*) is introduced to describe the acceleration times between the two processes.

$$AF(t_i) = \frac{t_i}{t_0} \tag{11}$$

Similarly, the entropy flow could be regarded as the equivalent of wear due to the linear relationship between them. By substituting the entropy function Equation (5) into Equation (10), the mathematical model of the accelerated wear test method based on the dissipation wear model could be obtained, meaning that the two processes could be considered as equal when the same entropy flow S_f is reached, respectively, with a higher entropy increase rate $\dot{S}_{fi}$ by shorter duration t_i under higher duty parameters and with lower entropy increase rate $\dot{S}_{f0}$ by longer duration t_0 under common duty parameters.

$$\dot{S}_{fi} \cdot t_i = \dot{S}_{f0} \cdot t_0 \tag{12}$$

The acceleration effect could be estimated by *AF* based on Equations (8) and (11).

$$AF(t_i) = \frac{t_i}{t_0} = \frac{\dot{S}_{f0}}{\dot{S}_{fi}} = \frac{\xi_0 \mu_0 N_0 v_0}{\xi_i \mu_i N_i v_i} \frac{T_i}{T_0} \tag{13}$$

To sum up, the theoretical basis of the accelerated wear test based on the dissipation wear model as well as the estimation approach are proposed in this section.

2.3. Design Based on Entropy Gradient

2.3.1. Gradient of Entropy Increase Rate

It is revealed in Section 2.2 that the wear test duration could be shortened by adjustment of the entropy increase rate, so that selecting the appropriate duty parameter to adjust is an important issue, since the entropy increase rate $\dot{S}_f$ in a wear system is decided by several parameters; see Equation (14).

$$\dot{S}_f = \xi \frac{\mu N v}{T_{bulk}} \tag{14}$$

According to Equations (10) and (14), the friction coefficient μ and the load-sharing factor ξ could be regarded as functions of the Hersey parameter G of the Stribeck curve.

$$\mu = \mu(G) \tag{15}$$

$$\xi = \xi(G) \tag{16}$$

Thus, the entropy increase rate $\dot{S}_f$ could be expressed as a function of the Hersey parameter G and the sliding velocity v, the normal load N and the temperature T.

$$\dot{S}_f(G, N, v, T) = \xi(G)\mu(G)\frac{Nv}{T} \tag{17}$$

In Equation (17), the Hersey parameter G is a function of the sliding velocity v, the normal load N and the temperature T if the viscosity η is defined as a function of the temperature with a Barus viscosity–temperature equation.

$$G(N, v, T) = \frac{\eta(T)v}{N} \tag{18}$$

$$\eta(T) = \eta_0 \exp(\beta(T - T_0)) \tag{19}$$

With Equations (17)–(19), $\dot{S}_f$ is a function of the sliding velocity v, the normal load N and the temperature T.

$$\dot{S}_f = \dot{S}_f(N, v, T) = \xi(G(N, v, T))\mu(G(N, v, T))\frac{Nv}{T} \tag{20}$$

To investigate the acceleration effect of each parameter on the entropy increase rate $\dot{S}_f$ and decide which parameter to be adjusted to accelerate the wear tests, the gradient of each parameter is obtained as follows.

For the sliding velocity v:

$$\frac{\partial \dot{S}_f}{\partial v} = \frac{\eta v^2}{T}\left(\frac{\mathrm{d}\dot{S}_f}{\mathrm{d}\xi}\frac{\mathrm{d}\xi}{\mathrm{d}G}\mu + \frac{\mathrm{d}\dot{S}_f}{\mathrm{d}\mu}\frac{\mathrm{d}\mu}{\mathrm{d}G}\xi\right) + \xi\mu\frac{N}{T} \tag{21}$$

For the normal load N:

$$\frac{\partial \dot{S}_f}{\partial N} = -\frac{1}{2N}\frac{\eta v^2}{T}\left(\frac{\mathrm{d}\dot{S}_f}{\mathrm{d}\xi}\frac{\mathrm{d}\xi}{\mathrm{d}G}\mu + \frac{\mathrm{d}\dot{S}_f}{\mathrm{d}\mu}\frac{\mathrm{d}\mu}{\mathrm{d}G}\xi\right) + \xi\mu\frac{v}{T} \tag{22}$$

For the temperature T:

$$\frac{\partial \dot{S}_f}{\partial T} = -\beta e^{-\beta(T-T_0)}\frac{v^2}{T}\left(\frac{\mathrm{d}\dot{S}_f}{\mathrm{d}\xi}\frac{\mathrm{d}\xi}{\mathrm{d}G}\mu + \frac{\mathrm{d}\dot{S}_f}{\mathrm{d}\mu}\frac{\mathrm{d}\mu}{\mathrm{d}G}\xi\right) - \xi\mu\frac{Nv}{2T^2} \tag{23}$$

2.3.2. Design Steps

Based on the analysis in Section 2.3.1, the design steps of the accelerated wear tests could be suggested.

Step 1: The Stribeck curve of the tribo-pair should be obtained; thus, the function $\xi(G)$ and $\mu(G)$ are obtained. Both μ and ξ could be expressed as a linear equation of G considering that the friction coefficient μ is approximately a linear function of G under mixed lubrication [43–45]; meanwhile, the load-sharing factor ξ is regarded as an interpolation result of μ (see Equation (10)).

$$\mu = k_1 G(N, v, T) + b_1 \tag{24}$$

$$\xi = k_2 G(N, v, T) + b_2 \tag{25}$$

Step 2: The Hersey parameter G_0 at the common duty condition should be set as the beginning point, and the aimed AF should also be set.

Step 3: The gradient of the entropy increase rate $\dot{S}_f$ with the sliding velocity v, the normal load N and the temperature T should be calculated, respectively, through the Stribeck curve at the present G. The entropy increase rate $\dot{S}_f$ could be completely written as a function of N, v and T with Equations (24) and (25).

$$\dot{S}_f(N, v, T) = k_1 k_2 \frac{\eta^2 v^3}{NT} + (k_1 b_2 + k_2 b_1)\frac{\eta v^2}{T} + b_1 b_2 \frac{Nv}{T} \tag{26}$$

The gradient of the entropy increase rate $\dot{S}_f$ by each parameter (see Equations (21)–(23)) could be further expressed as Equations (27)–(29).

$$\frac{\partial \dot{S}_f}{\partial v} = 3k_1 k_2 \frac{\eta^2 v^2}{NT} + 2(k_1 b_2 + k_2 b_1)\frac{\eta v}{T} + b_1 b_2 \frac{N}{T} \tag{27}$$

$$\frac{\partial \dot{S}_f}{\partial N} = -k_1 k_2 \frac{\eta^2 v^3}{2N^2 T} + b_1 b_2 \frac{v}{T} \tag{28}$$

$$\frac{\partial \dot{S}_f}{\partial T} = -k_1 k_2 (2\beta + 1) \frac{e^{-2\beta(T-T_0)} v^3}{NT} - (k_1 b_2 + k_2 b_1)(\beta + 1) \frac{e^{-\beta(T-T_0)} v^2}{T} - b_1 b_2 \frac{Nv}{2T^2} \quad (29)$$

Step 4: The three gradients calculated in step 3 should be compared; then, the wear test will be accelerated in the largest gradient direction to acquire the fastest acceleration effect.

Step 5: A new accelerated Hersey parameter G_i is reached with the adjustment of v, N or T, the $\dot{S}_{fi}$ should be calculated to judge if the aimed AF is reached.

Theoretically, the accelerated entropy increase rate $\dot{S}_{fi}$ at the accelerated Hersey parameter G_i could be obtained by an integral calculation.

$$\dot{S}_{fi} = \dot{S}_{f0} + \int_{G_0}^{G_i} \frac{\mathrm{d}\dot{S}_f}{\mathrm{d}G} \mathrm{d}G \quad (30)$$

The accelerated entropy increase rate $\dot{S}_{fi}$ could be approximately estimated with differential calculation, in which the ΔG is defined by adjustment of v, N or T.

$$\dot{S}_{fi} = \dot{S}_{f0} + \left. \frac{\mathrm{d}\dot{S}_f}{\mathrm{d}G} \right|_{G=G_0} \Delta G \quad (31)$$

Step 6: Step 3 to step 5 should be repeated until the aimed AF is reached. The final accelerated entropy increase rate $\dot{S}_{fn}$ will be an accumulation value of each acceleration step.

$$\dot{S}_{fn} = \dot{S}_{f0} + \sum_{i=0}^{n-1} \left. \frac{\mathrm{d}\dot{S}_f}{\mathrm{d}G} \right|_{G=G_i} \Delta G_i \quad (32)$$

The algorithm flow diagram is shown as Figure 1a; more detailed steps are shown on a Stribeck curve in Figure 1b.

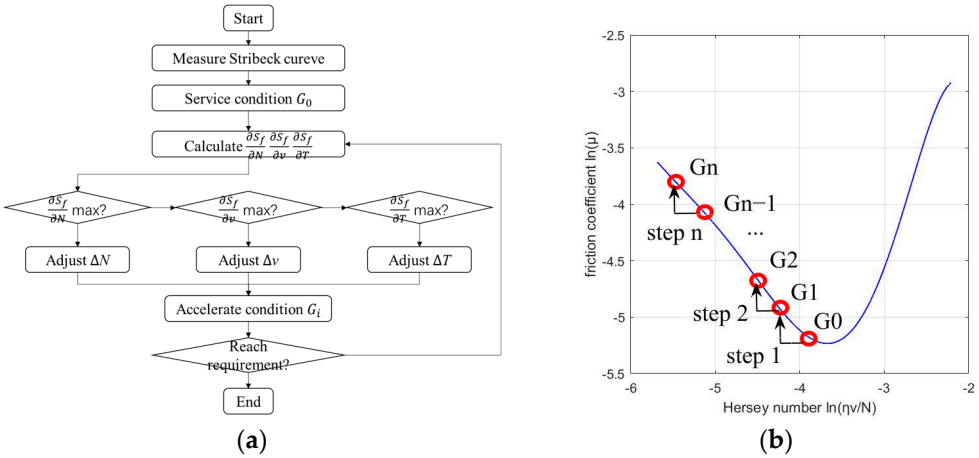

Figure 1. Theoretical design process of the accelerated wear test: (**a**) The algorithm flow diagram of the accelerated wear test; (**b**) Design step for the accelerated wear test by steps.

3. Experimental Verification

In this section, an example of an accelerated wear test is conducted to verify the method proposed in this paper. A stainless steel-graphite tribo-pair is tested on the Plint TE-92 standard tester (Phoenix Tribology, Kingsclere, UK) for wear experiment under mixed lubrication condition. The friction coefficient is calculated by the load and friction torque measured, respectively, by the load cell and torque sensor of the tester. The thermocouple of the tester could measure the temperature of the sample surface through a machined hole on the sample. The drawings of samples and tester are shown in Figure 2.

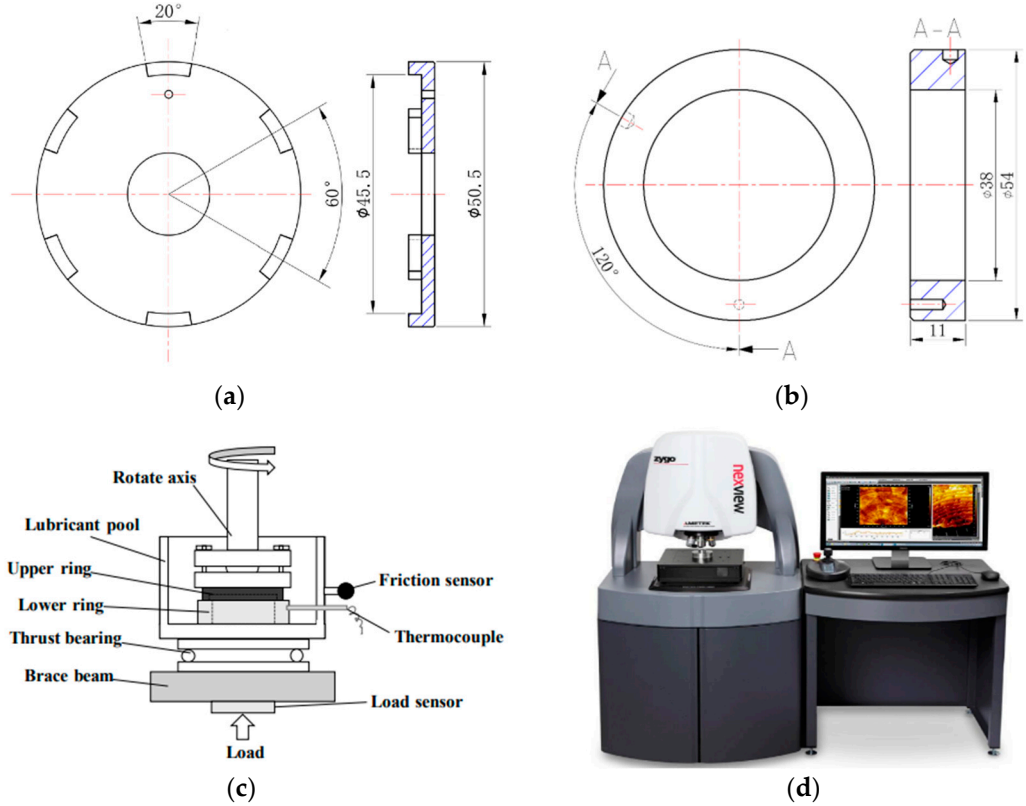

Figure 2. Drawings of samples and testers: (**a**) Upper sample; (**b**) Lower sample; (**c**) Plint TE-92 standard tester; (**d**) Zygo Nex View white light interferometer (Middlefield, CT, USA).

The results are obtained from the Zygo Nex View white light interferometer by measuring the average depth of the wear scratch. The wear amount is presented by the soft graphite material volume wiped off by the opposite hard stainless steel material in the wear process, while the wear rate is defined as the ratio of wear volume and total wear distance.

$$w_v = 2\pi r_m hb \tag{33}$$

$$\dot{w}_v = \frac{2\pi r_m hb}{2\pi r_m R_{ev}} = \frac{hb}{R_{ev}} \tag{34}$$

3.1. Dissipation Wear Model Verification

The Stribeck curve of the tribo-pair is measured firstly to determine the duty parameter range of the mixed lubrication regime, since such a range is required to calculate the load-sharing factors. The test parameters and corresponding results for the Stribeck curve are shown in Table 1, while the calculated load-sharing factors are shown in Table 2.

Table 1. Test parameters and corresponding results of the Stribeck curve measurement.

Test Order Number	Sliding Velocity/(m/s)	Load/N	Temperature/°C	Hersey Parameter	Friction Coefficient
1	0.14	399.99	32.27	0.012	0.059
2	0.095	399.91	24.33	0.010	0.078
3	0.071	399.95	25.94	0.0073	0.071
4	0.047	399.93	25.52	0.0049	0.074
5	0.14	800.03	30.25	0.0065	0.082
6	0.094	799.98	30.89	0.0042	0.085

Table 2. Results of the calculated load-sharing factor.

Test Order Number	Condition Parameter	Friction Coefficient	Load Sharing Factor
1	0.012	0.059	0
2	0.010	0.078	0.73
3	0.0073	0.071	0.45
4	0.0049	0.074	0.59
5	0.0065	0.082	0.89
6	0.0042	0.085	1

The dissipation wear model under mixed lubrication conditions is verified by a series of standard wear tests, of which the entropy increase rate in the contact area is obtained by Equation (14) and the parameters in Tables 1 and 2. Results data are shown in Table 3.

Table 3. Results of verification test for the dissipation model under mixed lubrication.

Test Order Number	Entropy Increase Rate in Contact Area/(J/(K·s))	Wear Rate by Distance/mm^2
1	0	0.26
2	0.0073	0.89
3	0.003	0.49
4	0.0028	0.61
5	0.028	2.36
6	0.021	1.93

From the data in Table 3, a remarkable linear relationship (see Equation (35)) could be revealed from the fitted function between the wear rates and the entropy increase rates in the contact area; see Figure 3.

$$\dot{w}_v = 74.5824\dot{S}_f + 0.3181 \tag{35}$$

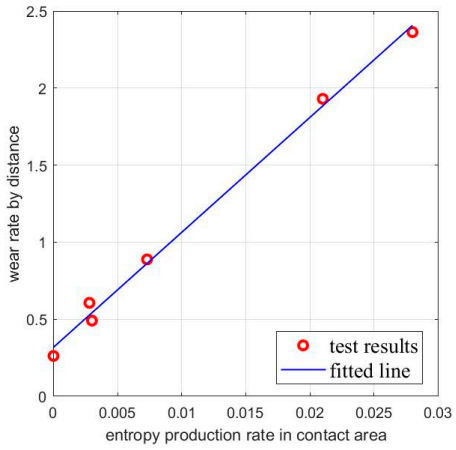

Figure 3. Test results and fitted function of the dissipation wear model.

In summary, the expected linear relationship of the dissipation wear model under mixed lubrication conditions is verified in this section.

3.2. Accelerated Wear Test Verification

With the verification of the model above, the entropy increase could be regarded as an equivalent of wear amount under mixed lubrication conditions. On this basis, a series of further standard tests are conducted to verify the accelerated wear test method suggested in Section 2.2.

Under the same entropy increase amount that corresponds to the equal wear effect, a group of accelerated wear tests with different expected test durations and inversely proportional entropy increase rates are designed with different duty parameters, as shown in Table 4.

Table 4. Parameters of verification test for accelerated wear test method.

Test Order Number	Sliding Velocity/(m/s)	Load/N	Temperature/°C	Entropy Increase Rate in Contact Area/(J/(K·s))	Expected Duration/min
1	0.14	400	40	1.26×10^{-3}	10
2	0.29	400	40	5.42×10^{-4}	26
3	0.34	400	40	1.96×10^{-4}	41
4	0.39	400	40	2.95×10^{-4}	93
5	0.43	400	40	6.35×10^{-5}	200

Each test will be conducted under the set duty parameters for the expected duration; then, wear depth will be measured to calculate the wear amount. The feasibility of the proposed method is estimated by comparing the obtained wear amounts under different entropy increase rates.

As shown in Figure 4, acceptable errors of the test results are obtained between tests with different duty parameters, revealing that the accelerated wear test method based on a dissipation wear model could be used to shorten the wear test duration. The largest acceleration time in these test is 20, with a relative error of wear amount less than 5%.

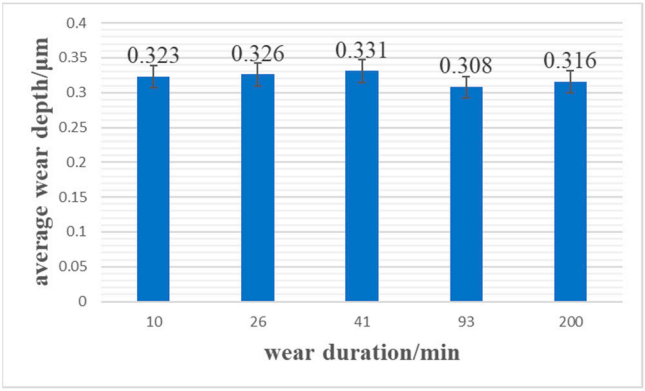

Figure 4. Results of the accelerated wear tests under different entropy increase rates.

3.3. Discussion of Linear Fitting

The sliding velocity is selected as the adjustment parameter to accelerate the tests in Section 3.2. Here, the basis of such selection will be discussed, and a design method to decide the fastest acceleration parameter by entropy gradient analysis will be proposed.

By substituting the data in Tables 1 and 2 into Equations (24) and (25), a fitted linear function could be obtained for the friction coefficient and the load-sharing factor, as shown in Figure 5.

The fitted $\mu - G$ function and $\xi - G$ function are shown as Equations (36) and (37).

$$\mu = -2.1674G + 0.0913 \tag{36}$$

$$\xi = -83.2004G + 1.2394 \tag{37}$$

It could be reveled from Figure 5 that there are considerable errors in the linear fitting; thus, the implication of such errors for the accelerated wear test will be discussed in this section.

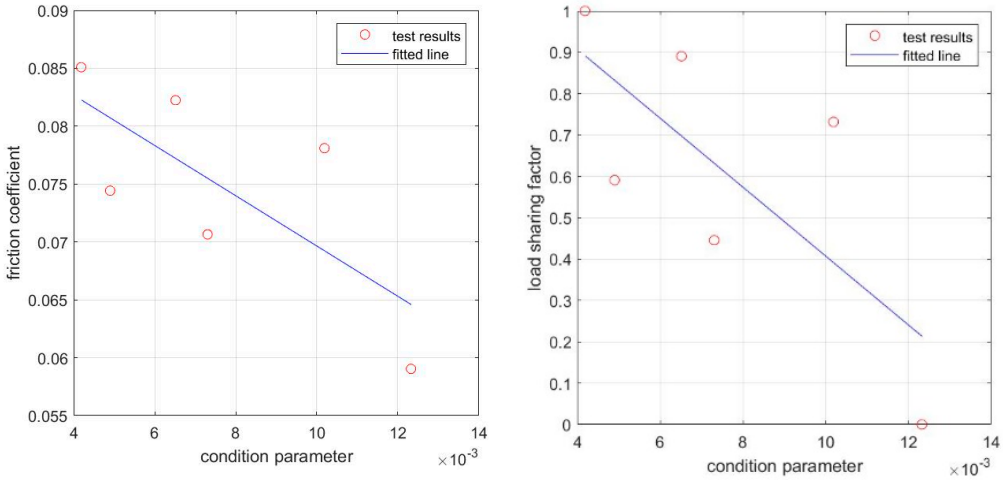

(**a**) (**b**)

Figure 5. Fitted linear functions of μ and ξ: (**a**) Fitted linear function of $\mu - G$; (**b**) Fitted linear function of $\xi - G$.

The interpolation method shown as Equation (9) could be presented as a $\mu_i - \xi_i$ linear function.

$$\xi_i = \frac{\xi_n - \xi_0}{\mu_n - \mu_0}\mu_i - \frac{\xi_n - \xi_0}{\mu_n - \mu_0}\mu_0 + \xi_0 = k_3\mu_i + b_3 \tag{38}$$

Since the value of $\xi_n = 1$ and the value of $\xi_0 = 0$, Equation (39) could be presented.

$$\xi_i = \frac{1}{\mu_n - \mu_0}\mu_i - \frac{1}{\mu_n - \mu_0}\mu_0 = k_3\mu_i + b_3 \tag{39}$$

If further simplification is conducted assuming that μ_0 closes to zero, the ξ_i would be in direct proportion with μ_i.

$$\xi_i = \frac{1}{\mu_n}\mu_i = k_3\mu_i \tag{40}$$

The relative error ε_ξ of load-sharing factor ξ_i could be correspondingly derived when there is a relative error ε_μ for friction coefficient μ_i.

$$\xi_i(1 + \varepsilon_{\xi i}) = k_3\mu_i(1 + \varepsilon_{\mu i}) \tag{41}$$

$$\varepsilon_{\xi i} = k_3\varepsilon_{\mu i} \tag{42}$$

The effect of such an error is shown in Equations (43) and (44).

$$\dot{S}_{fi} = \xi_i(1 + \varepsilon_{\xi i})\mu_i(1 + \varepsilon_{\mu i})\frac{N_i v_i}{T_i} = (1 + k_3\varepsilon_{\mu i})(1 + \varepsilon_{\mu i})\xi_i\mu_i\frac{N_i v_i}{T_i} \tag{43}$$

$$AF(t_i) = \frac{\dot{S}_{f0}}{\dot{S}_{fi}} = \frac{(1 + k_3\varepsilon_{\mu 0})(1 + \varepsilon_{\mu 0})\xi_0\mu_0 N_0 v_0}{(1 + k_3\varepsilon_{\mu i})(1 + \varepsilon_{\mu i})\xi_i\mu_i N_i v_i}\frac{T_i}{T_0} \tag{44}$$

The turning point of the Stribeck curve could be found with extended test, as shown in Figure 6. The μ_0 is an order of magnitudes less than μ_n, so that the assumption of Equation (40) could be satisfied.

Since the relative error of μ for the accelerated wear test in this paper are all close to the same value shown in Figure 7a, the error items in Equation (44) could be eliminated, so that the *AF* is basically accurate, although large errors exist in the linear fitting of Equations (36) and (37), as shown in Figure 7b; the detailed data are listed in Table 5. Such insensitivity of *AF* to error is an advantage of the accelerated wear test method proposed in this paper. However, the prediction of wear still requires accurate measurement and

calculation of friction coefficient μ and load-sharing factor ξ, which will be a significant issue in further investigations.

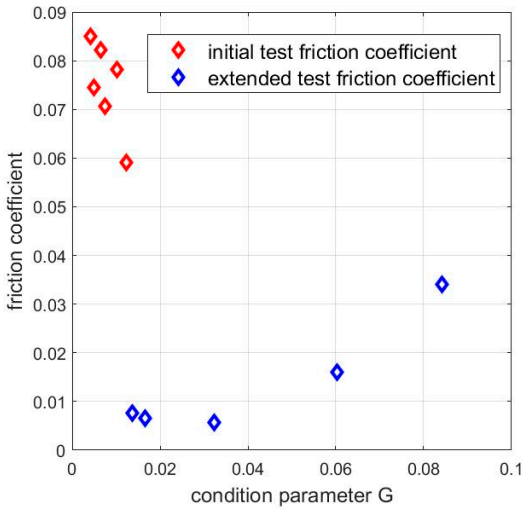

Figure 6. Extended Stribeck curve.

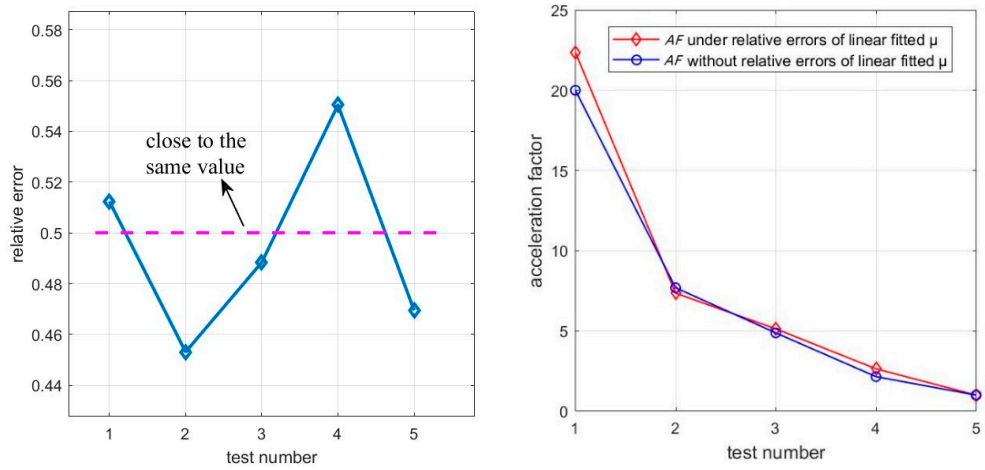

(**a**) (**b**)

Figure 7. Implication of errors of linear fitted friction coefficient μ on accelerated factor: (**a**) Relative errors of μ; (**b**) *AF* under errors.

Table 5. Acceleration factor for the accelerated wear test under relative error of μ.

Accelerated Test Number	Duration/min	Measured μ	Equation (36) Fitted μ	*AF* with Error	*AF* without Error
1	10	0.143	0.0697	22.366	20
2	26	0.088	0.0481	7.355	7.692
3	41	0.08	0.0409	5.129	4.878
4	93	0.075	0.0337	2.639	2.151
5	200	0.05	0.0265	1	1

3.4. Discussion of Entropy Gradient

Among the duty parameters that decide the value of *G*, few changes have been observed from the temperature with the change of *G* in repeated tests for measurement of the Stribeck curve under mixed lubrication, as shown in Figure 8.

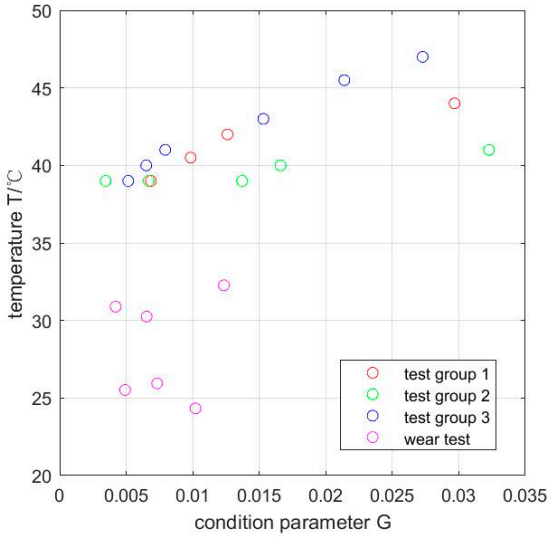

Figure 8. Temperatures of different condition parameters under mixed lubrication.

Hence, the temperature could be concerned as a constant for tests in this paper so that the entropy increase rate could be simplified as a function with double variants: the sliding velocity v and the normal load N. With Equations (36) and (37), the entropy increase rate $\dot{S}_f$ could be expressed quantitatively.

$$\dot{S}_f(N, v) = 881.6363\frac{v^3}{N} - 1.3089v^2 + 3.7507 \times 10^{-4}Nv \tag{45}$$

Additionally, the relationship between entropy increase rate $\dot{S}_f$ with the sliding velocity v and the normal load N could be further expressed on a 3D surface, from which it could be revealed that $\dot{S}_f$ would have an accelerated increase with the increasing normal load and the decreasing sliding velocity.

Equations (27) and (28) could be expressed quantitatively so that the gradient of Figure 9 could be obtained, revealing the changing speed of the entropy increase rate with the sliding velocity and the normal load.

$$\frac{\partial \dot{S}_f}{\partial v} = 2648\frac{v^2}{N} - 2.6209v + 3.755 \times 10^{-4}N \tag{46}$$

$$\frac{\partial \dot{S}_f}{\partial N} = -441.3303\frac{v^3}{N^2} + 3.755 \times 10^{-4}v \tag{47}$$

If the load is set as different values around the test normal load, the gradient $\partial \dot{S}_f / \partial v$ could be calculated. Similarly, if the sliding velocity is set as different values around the test rotating speed, the gradient $\partial \dot{S}_f / \partial N$ could be calculated, as shown in Figure 10.

It could be revealed from the comparison of the two gradients that the gradient by the sliding velocity is three orders of magnitudes larger than that by the normal load, so that a remarkably better acceleration effect could be obtained by adjusting the sliding velocity of the example in this paper, proving that the sliding velocity adjustment operation in Section 3.2 is appropriate.

Although sliding velocity adjustment is the suitable direction for the accelerated wear test, there is a restricted range in which the gradient by sliding velocity is negative so that the entropy increase rate could be increased. In this paper, the acceleration sliding velocity range is (0.14 m/s, 0.36 m/s); see Figure 11a. With the sliding velocity decreasing in such a range, the *AF* will increase from 1 to 20; see Figure 11b.

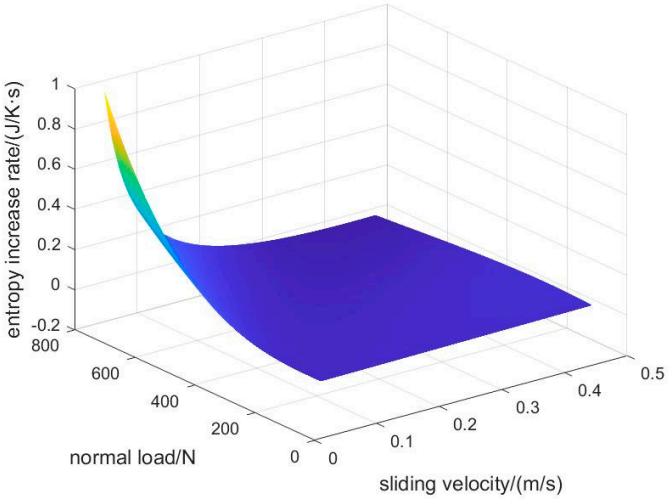

Figure 9. Surface plot of the entropy increase rate with sliding velocity and normal load.

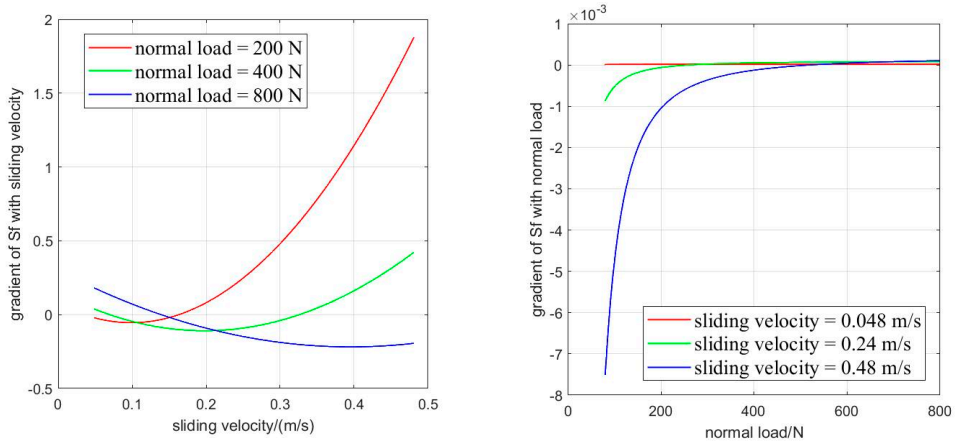

(**a**) (**b**)

Figure 10. Gradients of $\dot{S}_f$ by different duty parameters: (**a**) Gradient of $\dot{S}_f$ with sliding velocity under different loads; (**b**) Gradient of $\dot{S}_f$ with load under different sliding velocities.

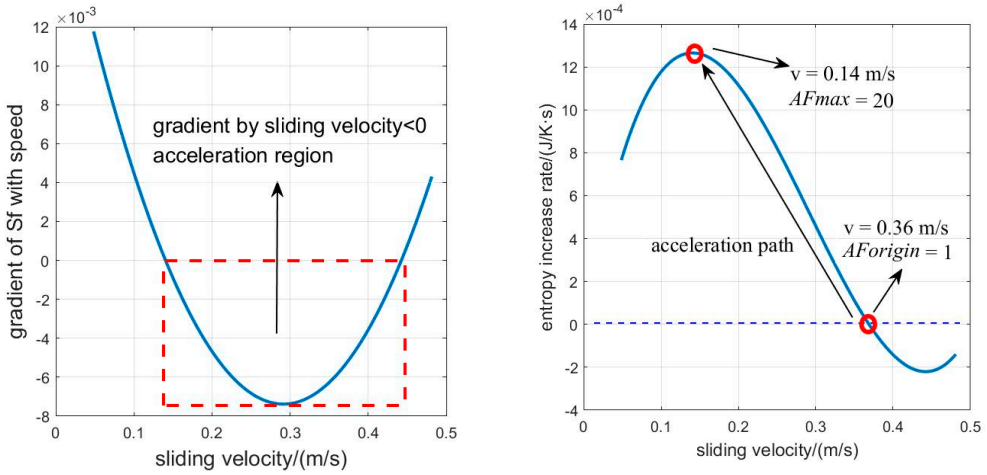

(**a**) (**b**)

Figure 11. Acceleration range by adjustment of speed: (**a**) The range shown in the gradient function; (**b**) The range shown in the entropy increase rate function.

The design process of the accelerated wear test suggested in Equation (32) is practiced with the test results in this paper. The acceleration step length is set as 10 rpm, and the corresponding entropy increase rates calculated by differential calculation for each step are presented in Figure 12. By comparison with the entropy increase rate predicted by Equation (45), it is revealed that the design method for the accelerated wear test by entropy gradient analysis and entropy increase rate predicted by Equation (32) is practicable.

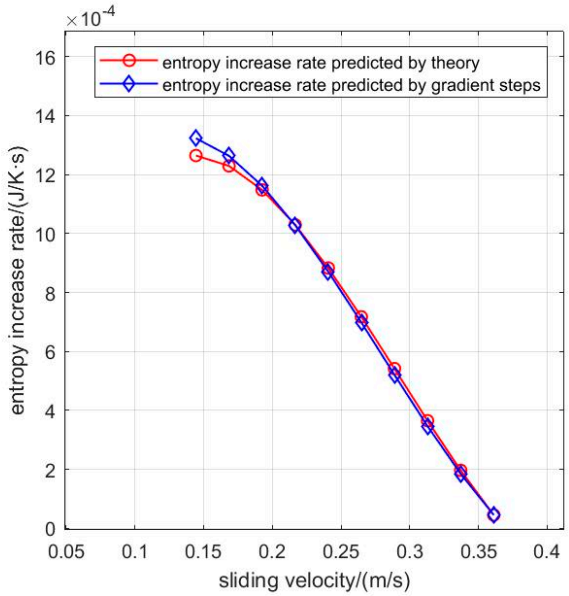

Figure 12. Comparison of predicted entropy increase rates.

4. Comparison and Application

4.1. Comparison with Archard Model

Since the Archard model is generally used for adhesive wear prediction, it is significant to demonstrate the advantages of a dissipation wear model through application in accelerated wear tests. A comparison is conducted between acceleration factors (*AF*) obtained by the Archard model theoretically and acceleration factors obtained by the experimental results presented in Table 4 and Figure 4, together with the predicted values of the proposed accelerated wear test method based on the dissipation wear model under mixed lubrication. The results are shown in Figure 13, and detailed values are listed in Table 6.

Table 6. Acceleration factors obtained by entropy increase rate and the Archard model.

Test Number	*AF* by Experiment	*AF* by Entropy	*AF* by Archard
1	20.443038	20	4.161557858
2	7.93573515	7.6923077	3.237209302
3	5.10960173	4.8780488	3.162790697
4	2.09609364	2.1505376	3.174418604
5	1	1	1

The remarkable inaccuracy of *AF* is presented by the Archard model in a wear acceleration test, while the proposed accelerated wear test *AF* conforms to that of the experiment results. The results could be explained by a mathematical model and wear mechanism.

The typical mathematical model of Archard could be presented in Equation (48).

$$w_v = K\frac{N}{H}s = K\frac{N}{H}vt \tag{48}$$

Under mixed lubrication, the normal load in the Archard model should be modified with the load-sharing factor.

$$w_v = K\frac{\xi N}{H}s = K\frac{\xi N}{H}vt \tag{49}$$

Based on Equation (49), the AF of two wear processes under different condition parameters could be presented through the Archard model with the assumption that the wear coefficient K and the material coefficient H are considered the same within the parameter range in Table 4.

$$AF(t_i) = \frac{t_i}{t_0} = \frac{\xi_0 N_0 v_0}{\xi_i N_i v_i} \tag{50}$$

Compared with Equation (13), the temperature and friction coefficient, which are the main influence factors of wear, are not considered in AF derived by the Archard model, leading to serious error in wear prediction.

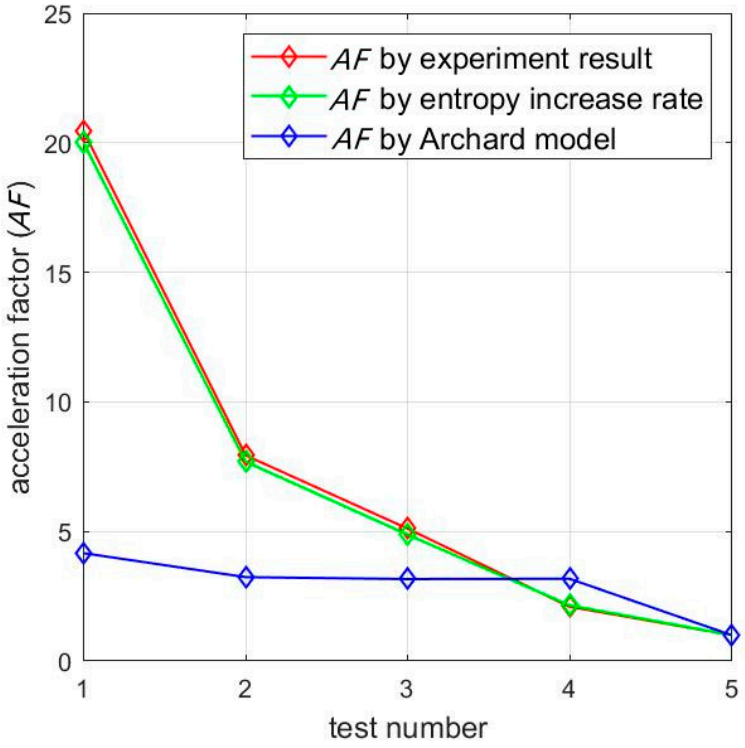

Figure 13. Comparison between AF obtained by entropy increase rate and the Archard model.

Such a mathematical view could be supported by wear mechanism analysis. Since only an adhesive wear mechanism is considered by the Archard model, other possible wear mechanisms are ignored. It is reported that wear prediction by only the Archard model could be inaccurate in multi-mechanism occasions [46]. Meanwhile, abrasive wear is common for typical stainless steel-graphite tribo-pairs such as that investigated in paper [47]. From the surface pictures in this paper shown in Figure 14, it could be revealed that the main wear mechanism would be abrasive wear where there are grooves and scratches on the friction surface. The view of thermodynamics that is involved in every kind of wear mechanism makes the dissipation wear model cover more wear mechanisms than the Archard model, thus gaining advantages in wear prediction and an accelerated wear test.

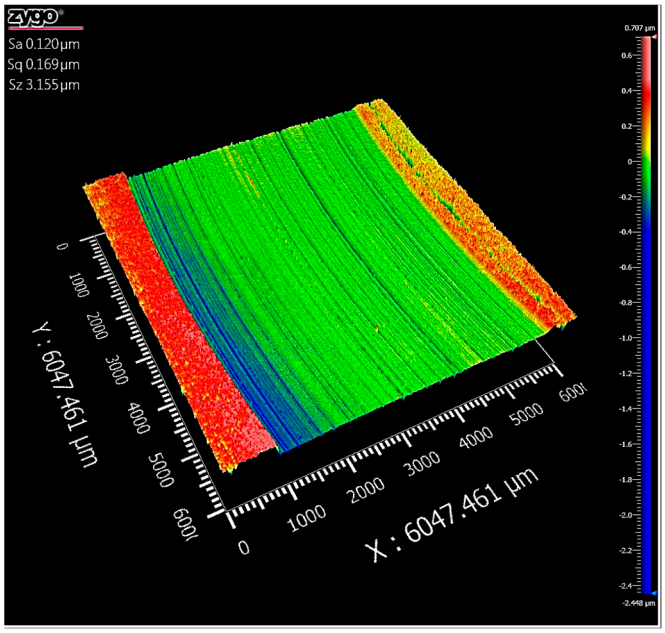

Figure 14. Picture of sample surface with grooves and scratches.

4.2. Application

To examine the practicability of the proposed method in severe working conditions, verification tests of the dissipation wear model and accelerated wear test method are conducted on a mechanical seal test bench. The stainless steel–graphite and Beryllium bronze–graphite seals are used as test samples. Schematic drawings of the samples and test bench are presented in Figure 15.

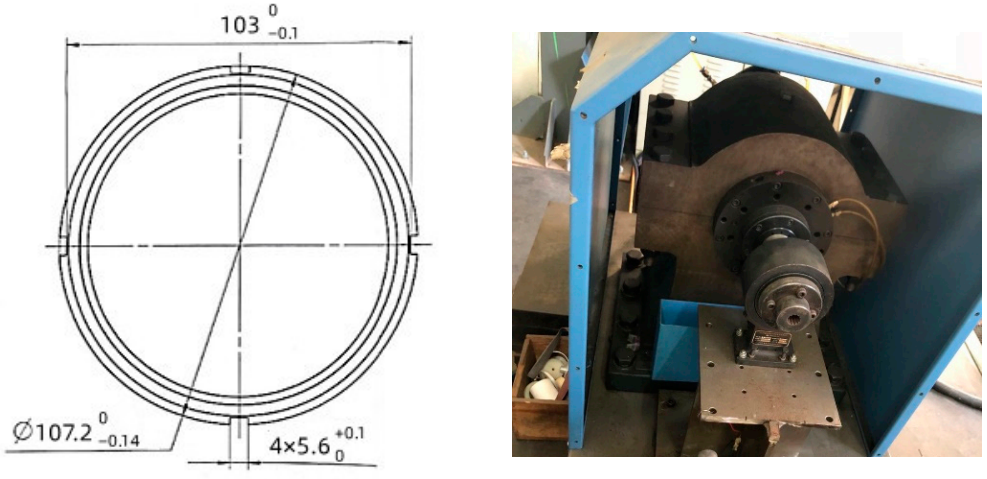

(**a**) (**b**)

Figure 15. Drawings of samples and picture of mechanical seal text bench: (**a**) Sample; (**b**) Test bench.

Since the friction coefficient could not be measured directly from the test, the entropy increase is calculated by the energy dissipation taken away by lubricants leakages. Such estimation based on temperature has been used by Doelling and Ling from a test that could not obtain the friction coefficient [39,40].

$$S_f = \frac{CM\Delta T}{T} \tag{51}$$

Although the experiment conditions and numbers are limited, a linear relationship could be obtained between the wear volume and entropy increase, as shown in Figure 16, and detailed values are listed in Table 7.

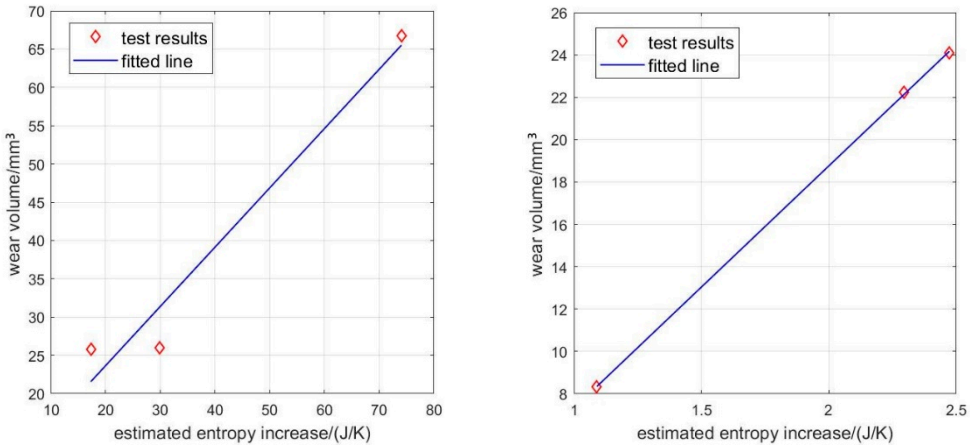

Figure 16. Test results and fitted function of the dissipation wear model under severe working condition: (**a**) Stainless steel–graphite; (**b**) Beryllium bronze–graphite.

Table 7. Results of severe working condition test for the dissipation model under mixed lubrication.

Test Number	Temperature/°C	Leakage/mL	Entropy Increase/(J/K)	Wear Volume/mm^3
steel-1	163.9	110.65	74.107	66.71112
steel-2	145.5002	49.35	29.93369	25.94321
steel-2	156.6122	26.8	17.29575	25.75791
bronze-1	142.1207	4.1625	2.473963	24.09013
bronze-2	147.1482	3.75	2.296664	22.23704
bronze-3	140.5241	1.85	1.088736	8.33889

According to the dissipation wear model verified, the accelerated wear test method could also be applied with entropy increase as a wear equivalent. Table 8 shows the accuracy of the predicted *AF*.

Table 8. Results of severe working condition accelerated wear test.

Test Number	Sliding Velocity/(m/s)	Normal Load/N	Entropy Increase/(J/K)	Predicted *AF*	Wear Volume/mm^3	Test *AF*
steel-2	37.722	1111.852	29.93369	1	25.943	1
steel-1	47.152	1111.852	74.107	2.476	66.711	2.571

The present experiment has preliminarily verified the feasibility of the acceleration method proposed in this paper. It is oriented to practical application and needs to be further studied.

5. Conclusions

The key for the design of an accelerated wear test is the decision of an appropriate equivalent of wear. Based on the dissipation wear model under mixed lubrication, this paper proposes a design method that considers the entropy increase as an equivalent of wear and accelerates by adjusting the entropy increase rate. Several conclusions have been reached as follows:

(1) The dissipation wear model under mixed lubrication is verified on a standard rotating wear tester. A linear relationships both between the wear amount and entropy increase amount, and between the wear rate and entropy increase rate, are obtained.
(2) A design method for an accelerated wear test under mixed lubrication is proposed based on the proved linear relationship by the dissipation wear model. The entropy increase is considered as an equivalent of wear amount. The acceleration effect is realized by increasing the entropy increase rate, which is inversely proportional with the test duration under the same entropy increase amount. A 20 times acceleration effect is reached in the verification test.
(3) Since the entropy increase rate is decided by duty parameters including sliding velocity, normal load and temperature, the relationship between acceleration effect and these duty parameters is analyzed based on the entropy increase rate gradients discussed. The results show that the fastest acceleration direction could be decided by adjusting the duty parameter of which the entropy increase rate gradient has the largest value.
(4) By comparison with the Archard model and application in severe working conditions, the advantages of the proposed accelerated wear test method are revealed.
(5) Although the acceleration factor of the proposed method possesses an insensitivity to error, the accuracy of measurement and calculation for friction coefficient μ and load-sharing factor ξ remain to be further investigated.

Author Contributions: Conceptualization, H.L. (Hongju Li) and Y.L.; data curation, H.L. (Hongju Li); investigation, H.L. (Hongju Li), H.L. (Haoran Liao) and Z.L.; methodology, H.L. (Hongju Li), H.L. (Haoran Liao) and Z.L.; software, H.L. (Hongju Li); validation, H.L. (Hongju Li), H.L. (Haoran Liao) and Z.L.; formal analysis, H.L. (Hongju Li); writing—original draft preparation, H.L. (Hongju Li); writing—review and editing, H.L. (Hongju Li), Y.L., H.L. (Haoran Liao) and Z.L.; visualization, H.L. (Hongju Li) and H.L. (Haoran Liao); supervision, Y.L.; project administration, Y.L.; resources, Y.L.; funding acquisition, Y.L. All authors have read and agreed to the published version of the manuscript.

Funding: This work was supported by the National Natural Science Foundation of China (51975315) and Major National R&D Projects/J2019-IV-0020-0088.

Institutional Review Board Statement: Not applicable.

Informed Consent Statement: Not applicable.

Data Availability Statement: The data that support the findings of this study are available from the corresponding author, Y.L. upon reasonable request.

Conflicts of Interest: The authors declare no conflict of interest. The funders had no role in the design of the study; in the collection, analyses, or interpretation of data; in the writing of the manuscript, or in the decision to publish the results.

Nomenclature

$\dot{S}$	entropy production rate
$\dot{S}_{gen}$	entropy source rate
$\dot{S}_f$	entropy flow rate
U	mess center velocity of material
J_q	density of heat flow
J_i	diffusion flow
Π	interfacial stress tensor
A_χ	chemical affinity
$\nu_{i\rho}$	stoichiometric coefficient
ω_χ	reaction speed
$\dot{w}_v$	volume wear rate
B	linear coefficient of dissipation wear model
$\dot{Q}$	heat condition

T_{bulk}, T	substrate temperature
μ	friction coefficient
N	normal load
v	sliding velocity
ξ	load-sharing factor
ξ_n, ξ_0, ξ_i	load-sharing factor at boundary-mixed transforming point, mixed-hydrodynamic transforming point and mixed lubrication condition
μ_n, μ_0, μ_i	friction coefficient at boundary-mixed transforming point, mixed-hydrodynamic transforming point and mixed lubrication condition
E_i, E_0	higher stress level equivalent function, common stress level equivalent function
t_i, t_0	higher stress level test duration, common stress level test duration
$\dot{S}_{fi}$, $\dot{S}_{f0}$	higher stress level entropy production rate, common stress level entropy production rate
G	the Hersey parameter
η, η_0	viscosity, viscosity under ambient condition
β	coefficient of Barus viscosity-temperature
T_0	temperature under ambient condition
k_1, k_2	$\mu - G$ function slope, $\xi - G$ function slope
b_1, b_2	$\mu - G$ function intercept, $\xi - G$ function intercept
G_i, G_0	accelerated Hersey parameter, initial Hersey parameter
$\dot{S}_{fn}$	final accelerated entropy production rate
w_v	volume wear amount
r_m	average radius of experimental sample
h, b	wear scratch depth, wear scratch width
R_{ev}	rotating cycles of test
C	specific heat capacity
M	leakage mass
ΔT	temperature rise
K	wear coefficient of Archard model
H	hardness coefficient of Archard model
k_3	$\mu_i - \xi_i$ function slope
b_3	$\mu_i - \xi_i$ function intercept

References

1. Sutharshan, B.; Mutyala, M.; Vijuk, R.P.; Mishra, A. The AP1000TM Reactor: Passive Safety and Modular Design. *Energy Procedia* **2011**, *7*, 293–302. [CrossRef]
2. Li, Z.L.; Zhang, X.R.; Xu, X.F.; Wang, Q.H. Investigation on the failure of slip sealing ring of typical engine at high speed and high temperature. *Lubr. Eng.* **2016**, *41*, 119–121.
3. Vakis, A.I.; Yastrebov, V.A.; Scheibert, J.; Nicola, L.; Dini, D.; Minfray, C.; Almqvist, A.; Paggi, M.; Lee, S.; Limbert, G.; et al. Modeling and simulation in tribology across scales: An overview. *Tribol. Int.* **2018**, *125*, 169–199. [CrossRef]
4. Minet, C.; Brunetiere, N.; Tournerie, B. A deterministic mixed lubrication model for mechanical seals. *J. Tribol.—Trans. ASME* **2011**, *133*, 042203. [CrossRef]
5. Aghdam, A.B.; Khonsari, M.M. Prediction of wear in grease lubricated oscillatory journal bearings via energy-based approach. *Wear* **2014**, *318*, 188–201. [CrossRef]
6. Wang, Y.C.; Liu, Y.; Huang, W.F.; Guo, F.; Wang, Y.M. The Progress and Engineering Application of Theoretical Model for Mixed Lubrication. *Tribology* **2016**, *36*, 520–530.
7. Fang, C.D. Prospective Development of Aeroengines. *Aeroengine* **2004**, *1*, 1–5.
8. Dong, Y.F.; Huang, M.; Li, R.Q. Overview of the development of general aviation engines. *J. Xi'an Aeronaut. Univ.* **2017**, *35*, 8–13.
9. Wang, P.H.; Fan, B.Y.; Fu, H.M. Reliability assessment and life prediction of satellite propeller. *Chin. J. Aerosp. Dyn.* **2004**, *19*, 745–748.
10. Zhou, K.; Luo, T.Y.; Zhang, L.W. Overview of storage life prediction technology on rocket and missile. *Environ. Eng.* **2005**, *2*, 6–11.
11. Meng, H.C.; Ludema, K.C. Wear models and predictive equations: Their form and content. *Wear* **1995**, *181*, 443–457. [CrossRef]
12. Meng, H. *Wear Modeling: Evaluation and Categorization of Wear Models*; The University of Michigan: Ann Arbor, MI, USA, 1994.
13. Bryant, M.D.; Khonsari, M.M. Application of degradation-entropy generation theorem to dry sliding friction and wear. In Proceedings of the STLE/ASME International Joint Tribology Conference, Miami, FL, USA, 20–22 October 2008; pp. 1–3.
14. Bryant, M.D.; Khonsari, M.M.; Ling, F.F. On the thermodynamics of degradation. *Proc. R. Soc. Lond. A* **2008**, *464*, 2001–2014. [CrossRef]
15. Czichos, H. *Tribology: A Systems Approach to the Science and Technology of Friction, Lubrication, and Wear*; Elsevier: New York, NY, USA, 1978.
16. Klamecki, B.E. An entropy-based model of plastic-deformation energy-dissipation in sliding. *Wear* **1984**, *96*, 319–329. [CrossRef]

17. Klamecki, B.E. Energy-dissipation in sliding. *Wear* **1982**, *77*, 115–128. [CrossRef]
18. Klamecki, B.E. Wear—Entropy increase-model. *Wear* **1980**, *58*, 325–330. [CrossRef]
19. Zmitrowicz, A. A thermodynamical model of contact, friction and wear: I Governing equations. *Wear* **1987**, *114*, 135–168. [CrossRef]
20. Zmitrowicz, A. A thermodynamical model of contact, friction and wear: II Constitutive-equations for materials and linearized theories. *Wear* **1987**, *114*, 169–197. [CrossRef]
21. Zmitrowicz, A. A thermodynamical model of contact, friction and wear: III Constitutive-equations for friction, wear and frictional heat. *Wear* **1987**, *114*, 199–221. [CrossRef]
22. Aghdam, A.B.; Khonsari, M.M. On the correlation between wear and entropy in dry sliding contact. *Wear* **2011**, *270*, 781–790. [CrossRef]
23. Aghdam, A.B.; Khonsari, M.M. Prediction of wear in reciprocating dry sliding via dissipated energy and temperature rise. *Tribol Lett.* **2013**, *50*, 365–378. [CrossRef]
24. Zhang, G.L.; Liu, Y.; Wang, Y.C.; Liu, X.F. A Friction-Dissipation Based Method for Quantity Model and Prediction of Graphite/WC-Ni Wear under Dry Sliding. *Tribology* **2019**, *39*, 221–227.
25. Lijesh, K.P.; Khonsari, M.M. On the degradation of Tribo-components in boundary and mixed lubrication regimes. *Tribol. Lett.* **2018**, *67*, 1–11. [CrossRef]
26. Lijesh, K.P.; Khonsari, M.M. Application of thermodynamic principles in determining the degradation of tribo-components subjected to oscillating motion in boundary and mixed lubrication regimes. *Wear* **2019**, *436–437*, 203002. [CrossRef]
27. Mathew, M.C.; Mcclelland, G.M.; Erlandsson, R.; Chiang, S. Atomic-scale friction of a tungsten tip on a graphite surface. *Phys. Rev. Lett.* **1987**, *59*, 1942–1945.
28. Meyer, E.; Overney, R.; Brodbeck, D.; Howald, L.; Lüthi, R.; Frommer, J.; Güntherodt, H.-J. Friction and wear of Langmuir-Blodgett films observed by friction force microscopy. *Phys. Rev. Lett.* **1992**, *69*, 1777–1780. [CrossRef] [PubMed]
29. Kligerman, Y.; Etsion, I. Analysis of the hydrodynamic effects in a surface textured circumferential gas seal. *Tribol. Trans.* **2001**, *44*, 472–478. [CrossRef]
30. DiRusso, E. Design analysis of a self-acting spiral-groove ring seal for counter-rotating shafts. *J. Aircr.* **2013**, *21*, 618–622. [CrossRef]
31. Kumar, P.; Srivastava, V.K. Reciprocating sliding tribology of brake oil treated carbon fiber reinforced ceramic matrix composites. *Trans. Nonferrous Met. Soc. China* **2019**, *29*, 1903–1913. [CrossRef]
32. Chen, X.; Zhang, C.H. Research, Application and Development of Accelerated Testing. *J. Mech. Eng.* **2009**, *45*, 130–136. [CrossRef]
33. Deng, A.M.; Chen, X.; Zhang, C.H.; Wang, Y.S. A Comprehensive Review of Accelerated Degradation Testing. *ACTA Armamentarii* **2007**, *28*, 1002–1007.
34. Zhang, C.H.; Wen, X.S.; Chen, X. A Comprehensive Review of Accelerated Life Testing. *ACTA Armamentarii* **2004**, *25*, 485–490.
35. Nelson, W. Accelerated life testing-step-stress models and data analyses. *IEEE Trans. Reliab.* **1980**, *29*, 103–108. [CrossRef]
36. Nelson, W. Analysis of performance-degradation data from accelerated tests. *IEEE Trans. Reliab.* **1981**, *R-30*, 149–155. [CrossRef]
37. Meeker, W.Q.; Hamada, M. Statistical tools for the rapid development and evaluation of high-reliability products. *IEEE Trans. Reliab.* **1995**, *44*, 187–198. [CrossRef]
38. Yu, Q.P.; Sun, J.J.; Yu, B.; Ma, C.B. A fractal model of mechanical seal surfaces based on accelerating experiment. *Tribol. Trans.* **2017**, *60*, 313–323. [CrossRef]
39. Doelling, K.L.; Ling, F.F.; Bryant, M.D.; Heilman, B.P. An experimental study of the correlation between wear and entropy flow in machinery components. *J. Appl. Phys.* **2000**, *88*, 2999–3003. [CrossRef]
40. Ling, F.F.; Bryant, M.D.; Doelling, K.L. On irreversible thermodynamics for wear prediction. *Wear* **2002**, *253*, 1165–1172. [CrossRef]
41. Dai, Z.D.; Xue, Q.J. Progress and development in thermodynamic theory of friction and wear. *Sci. China Ser. E-Technol. Sci.* **2009**, *52*, 844–849. [CrossRef]
42. Dai, Z.D.; Wang, M.; Xue, Q.J. *Introduction to Tribothermodynamics*; National Defence Industry Press: Beijing, China, 2002.
43. Lu, X.B.; Khonsari, M.M.; Gelinck, E.R.M. The stribeck curve: Experimental results and theoretical prediction. *J. Tribol.* **2006**, *128*, 789–794. [CrossRef]
44. Akbarzadeh, S.; Khonsari, M.M. Effect of surface pattern on Stribeck curve. *Tribo Lett.* **2010**, *37*, 477–486. [CrossRef]
45. Lenning, R.L. The transition from boundary to mixed friction. *Lubr. Eng.* **1960**, 575–582.
46. Wang, Y.C. *Theoretical Model and Experimental Verification of Mixed Lubrication of Conformal Contact Surfaces*; Tsinghua University: Beijing, China, 2019.
47. Zhang, G.L.; Liu, Y.; Wang, Y.C.; Guo, F.; Liu, X.; Wang, Y. Wear behavior of WC-Ni sliding against graphite under water lubrication. *J. Mater. Sci. Technol.* **2017**, *33*, 1346–1352. [CrossRef]